CLM-R259

A measurement of the attenuation of optical fibres (fibres optiques QSF-W-600 μm) in the ultra violet region

A. R. Field
J. W. Thompson

UK ATOMIC ENERGY AUTHORITY

Culham Laboratory

CLM-R259

A Measurement of the Attenuation of Optical Fibres (Fibres Optiques QSF-W-600 μm) in the Ultra Violet Region

A.R. Field
J.W. Thompson

Culham Laboratory, Abingdon, Oxon, OX14 3DB, U.K.
(Euratom/UKAEA Fusion Association)

ABSTRACT

The attenuation of Fibres Optiques QSF-600-W optical fibres was measured in the wavelength range from 2300Å to 7000Å to assess their suitability for use on HBTX1A diagnostics.

The primary use intended for the fibres was to relay CV (2271Å) light to a spectrometer for multichord doppler ion temperature and plasma rotation measurements. Manufacturers data was available for the attenuation in the wavelength region 4000Å to 7000Å so the present work was undertaken to extend measurement into the region of 2200Å to 4000Å. The highest acceptable attenuation for the intended applications was 3.0dBm^{-1} and the highest measured attenuation was 3.8+/-1.0 dBm^{-1} at 2300Å confirming their suitability for this purpose.

Culham Laboratory
United Kingdom Atomic Energy Authority
Abingdon
Oxfordshire OX14 3DB

July 1987

ISBN:85311 161 8
Price:£4.00
Available from H.M. Stationery Office

THEORY

The optical fibre is a cylindrical dielectric waveguide for the directed transmission of electromagnetic waves at optical frequencies. The fibre type considered here was a step indexed type (Fibrosil QSF-600-W) with the refractive index varying as in Fig.1. A simple ray treatment gives a first insight into the mechanism of fibre transmission. Refering to Fig.2., rays entering the fibre at an angle A are guided by repeated total internal reflection at the refractive index drop at the core cladding interface. Meridional rays entering at an angle greater than A_0, the acceptance angle, related to the numerical aperture, NA, and refractive index by

$$NA = n_0 \sin A_0 = (n_1^2 - n_2^2)^{1/2} \qquad (1)$$

are lost from the core and absorbed in the P.T.F.E. coating and sheath. In (1), n_0 is the refractive index outside the fibre, n_1 the refractive index in the core and n_2 the refractive index in the cladding. Skew rays not intersecting the fibre axis can be transmitted to a degree dependent upon fibre symmetry.

The optical path length for a given fibre length depends upon the incident angle A, the maximum path length being for an incident angle A_0. This causes dispersion of a light pulse transmitted down a long fibre run.

Some light penetrates the sheath on reflection due to the evanescent part of the wave having a finite probability of being in the sheath, higher incident angle rays undergo more reflections and are therefore attenuated to a greater extent. Attenuation and dispersion can therefore be reduced at the expense of a reduced acceptance angle.

Attenuation mechanisms are of three types:-

i) End losses, not directly considered here as the measurement was of internal transmission and as end losses may be reduced using an index matching fluid.

ii) Scattering and absorption losses in the fibre core and cladding material.

iii) Geometrical effects on the light path.

Considering only internal attenuation, we must consider scattering and geometrical effects.

Scattering losses are of two types:-

i) Intrinsic scattering losses due to density fluctuations in the core, frozen in at manufacture, which cause Rayleigh scattering resulting in an attenuation, α, given by

$$\alpha = \frac{\text{const}}{\lambda 4} (n^2-1)KT_s$$

where n is the refractive index, λ the wavelength, K the isothermal compressibility and T_s the freezing temperature. This gives an attenuation of 0.4 dBm^{-1} at 2200Å, about 10^{-1} that measured (see [2]).

ii) Extrinsic scattering is due to impurity ions in the core, e.g. Fe^{3+}, Cu^{3+}, OH^-, inducing composition fluctuations causing Rayleigh scattering. The fibre considered here was of a 'wet' type with a comparatively high OH^- concentration. Absorption in the infra red due to excitation of vibrational modes of the OH^- ion is increased in 'wet' fibres but the short wavelength scattering is reduced. The impurity ions also increase absorption due to photon excitation of electrons into unfilled energy levels. This absorption mechanism is of primary importance in the ultra violet.

Geometrical anomalies such as faults in the cladding, bends, tapering and ellipsoidal cross section scatter the rays out of the range of optical paths transmitted by the fibre. The only geometrical variable under the control of the experimenter was bend radius, decreasing the bend radius decreases the numerical aperture and increases the attenuation, see [1,2]. The wave equations for $\underline{E}$ and $\underline{B}$ can be solved for the waveguide in the cylindrical approximation showing that the light propagates as discrete modes. The fibre considered here has a core radius very much greater than the wavelength leading to many closely spaced modes, higher order modes correspond to greater angles of propagation to the axis in the ray picture, geometrical and compositional anomalies can be shown to transfer energy between modes, ultimately to unconfined non-propagating modes leading to loss, see [2] for a discussion of this complex treatment.

THEORY OF THE METHOD

Consider a length of fibre, length L_1, with end transmissions T_1, T_{11}. The scattering losses may be considered using a simple exponential scattering law if it is assumed that scattering and absorption events occur at mean separations much less than the fibre

length. Giving, with an incident intensity I_0, a transmitted intensity, I_1

$$I_1 = I_0 T_1 T_{11} e^{-\alpha L_1} \qquad (2)$$

with I_0, I_1, T_1, T_{11} and α the attenuation coefficient, all functions of wavelength and α dependent on fibre material and geometry.

A second longer fibre of length L_2, illuminated under the same conditions with light levels measured by the same detector as fibre 1, gives

$$I_2 = I_0 T_2 T_{22} e^{-\alpha L_2} \qquad (3)$$

Combining (1) and (2) gives

$$\alpha = \frac{1}{L_2 - L_1} \left(\ln \left(\frac{I_1}{I_2} \right) - \ln \left(\frac{T_1 T_{11}}{T_2 T_{22}} \right) \right) \qquad (4)$$

with α_{db} in dB/unit length given by $\alpha_{db} = 10 \log_{10}(e^{\alpha})$.

If end losses were quantified the attenuation could be found from (4).

Manufacturers data gives an attenuation of 10 $dBkm^{-1}$ at 6500Å, a factor of 10^{-3} less than that measured at 2200Å.

Assuming α=0 at 6500Å would give from (4)

$$\frac{I_1}{I_2} = \frac{T_1 T_{11}}{T_2 T_{22}} \qquad (5)$$

enabling a measurement of $T_1 T_{11} / T_2 T_{22}$ to be made directly. This term is shown to be constant with wavelength to within the accuracy required in appendix.1.

METHOD

To measure the attenuation of the fibre using the principle outlined above it is necessary to illuminate fibres of differing lengths with monochromatic light, at various wavelengths covering the range of interest, under identical conditions for each fibre whilst holding the fibres at the same bend radius and then measure the light transmitted by each fibre with the same detector.

A mercury lamp has emission lines in the appropriate region, light from such a lamp being imaged onto the entrance slit of a Rank Hilger Monospek 1000 to select the lines required. All optics was either fused silica or $MgF\ell_2$ coated Aℓ with adequate transmission and reflection, for the purposes of the experiment, down to 2200Å.

Light from the exit slit is imaged onto the fibre ends by a fused silica lens, the f number of the incident cone being greater than that required to fully fill the acceptance cone of the fibre. The fibre accepts a 4Å bandwidth, sufficiently small for this investigation. Micrometer adjustment enables illumination of two fibres alternately under similar conditions.

Two fibres of length 0.925+/-0.001 m and 3.88+/-0.01 m are used, both bent around the same bend radius. The transmitted light from each fibre is measured using the same area of the cathode of a RCA 4840 photomultiplier with a quartz envelope, run at a dynode voltage low enough to ensure adequate linearity, a correction being made to each result by closing the spectrometer entrance slit and measuring the stray light and dark current at each condition. At the longer wavelengths diffused light from a HeNe laser (6529Å) is used as the Hg lamp is insufficiently bright in this region.

Below a setting of 2300Å the light from the monospec is contaminated with stray light at a longer wavelength. Glass filters with negligible transmission below 3500Å are used to measure only the stray light intensity, a correction being made to the measured intensity to take into account the absorption of the stray light in the filter, thus the intensity of the short wavelength transmitted light could be deduced after removal of the stray light component. The filter transmission is measured at the wavelength of the stray light using a region of stray light nearby uncontaminated with short wavelength lines.

RESULTS

Measurement of the transmitted light intensity for each fibre and wavelength, λ, $I_1(\lambda)$, $I_2(\lambda)$, corrected for stray light and dark current, along with measurement of the fibre lengths L_1, L_2 enables calculation of the attenuation, α, assuming that, as previously explained, $\alpha = 0.0$ at 6529Å. Treatment of errors from the measured uncertainties is explained in appendix.2. The results, corrected for end losses and errors, are shown in Fig.4. for 2304Å to 6529Å and in Fig.5. for 2304Å to 3200Å in dBm^{-1}. Manufacturers data for the QSF-W-600 fibre and similar fibres with different core diameters is shown in Fig.3. and Table.1.

CONCLUSIONS

The results presented here provide estimates of the attenuation of QSF-W-600 fibre over the wavelength range 2300Å to 6529Å where data were previously unavailable. Extrapolation down to 2271Å, where the fibres are intended to be used for doppler broadening measurements on CV(2271Å) in HBTX1A, gives an attenuation of $3.8+/-1.0dBm^{-1}$ marginally acceptable for the use intended.

ACKNOWLEDGEMENTS

We give our thanks to the support of Culham staff in completing this work, particularly Dr P.G.Carolan for his supervision and encouragement.

REFERENCES

[1] Fibre Optics, E.D.LACEY, Prentice Hall, 1982.

[2] Fibre Optics; devices and systems, P.K.Cheo, Prentice Hall, Series in Solid State Physical Electronics, 1985.

Treatment of the Wavelength Dependence of the End Losses

It is required to estimate the magnitude and wavelength dependence of end loss term $(T_1T_{11})/(T_2T_{22})$. The fibre ends could be seen to be plane perpendicular to the fibre axis to within 10°. Assuming we have two fibres with ends 5° and 10° from perpendicular, Fresnels equation gives

$$T_{12} = 1-(n_2\cos\Theta_1-n_1\cos\Theta_2)/(n_2\cos\Theta_1+n_1\cos\Theta_2) \qquad (6)$$

where T_{12} is the transmitted fraction on passing from media refractive index n_1 at incident angle to the normal Θ_1 into media refractive index n_2 at emergent angle Θ_2 to the normal. This enables calculation of $(T_1T_{11})/(T_2T_{22})$ at the two extremes used in the measurement.

The refractive indices of fused silica at these wavelengths are

$n(6300\text{Å}) = 1.45$
$n(2300\text{Å}) = 1.52$

If n_1 refers to the 10° fibre then calculation gives

$(T_1T_{11})/(T_2T_{22}) = 0.982$ at 2300Å and 0.984 at 6300Å.

This gives an insignificant variation in end losses with wavelength in comparison with the measurement errors. Other possible sources of end loss, e.g. obscured or chipped ends, should be constant with wavelength. End losses could therefore be considered a constant systematic error.

Treatment of Errors

Owing to the limited time available to carry out the experiment only two fibres were used, making a statistical treatment of errors and end losses impossible. The error treatment used here represents the propagation of measurement uncertainties only.

Errors were calculated for the attenuation by operating on (7) with the chain rule, (8).

$$\alpha = 10 \log_{10} e \, (1/(L_1 - L_2) \ln(I_1/I_2) + \text{const}) \tag{7}$$

$$d\alpha = (d\alpha/dL)\, dL + (d\alpha/df)df \tag{8}$$

where $f = I_1/I_2$, $L = L_1 - L_2$

giving

$$d\alpha = 10 \log_{10} e \, [1/(fL)\, df - \ell nf/(L^2) d\, L] \approx 10 \log_{10} [e \frac{df}{fL}] \tag{9}$$

The errors in L were so small as to make the second term in (9) negligible.

FIBRE TYPE		QSF-200-W	QSF-300-W	QSF-400-W	QSF-600-W	QSF-1000-W	QSF-1500-W
CORE DIAMETER (μm)		200	300	400	600	1000	1500
SHEATH DIAMETER (μm)		380	440	550	750	1250	1850
CORE/CLADDING ECCENTRICITY (μm)		20	20	20	25	30	30
COATING DIAMETER (μm)		600	650	850	1060	1550	2400
STANDARD LENGTHS (m)		1100(±5%)	1100(±5%)	500(±5%)	500±(5%)	-	-
		2500(±5%)	2500(±5%)	1100(±5%)			
MAXIMUM ATTENUATION	0.82μm	8	7	7	6	6	6
	0.63μm	15	12	12	10	10	10
NUMERICAL APERTURE	Theoretical	0.4	0.4	0.4	0.4	0.4	0.4
	Steady state	0.27	0.27	0.27	0.27	-	-
TYPICAL BANDWIDTH (MHz km)		20	18	15	9	-	-
WEIGHT (kg km^{-1})		0.49	0.61	1.05	1.75	3.6	8.5
TENSILE STRENGTH ($DaNmm^{-2}$)		35	32	32	32	32	32
STOCK DIAMETER (mm)		212	212	212	450	500	750

Table.1. A summary of manufacturers data for fibres of 200μm to 1500μm core diameters.

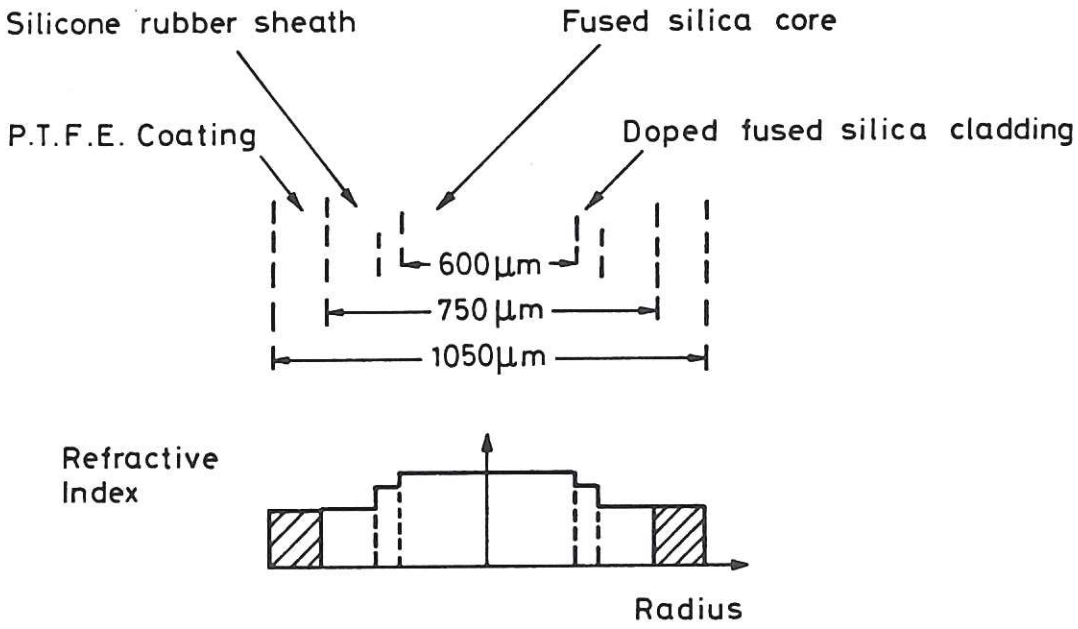

Fig.1. The profile of refractive index across the fibre diameter.

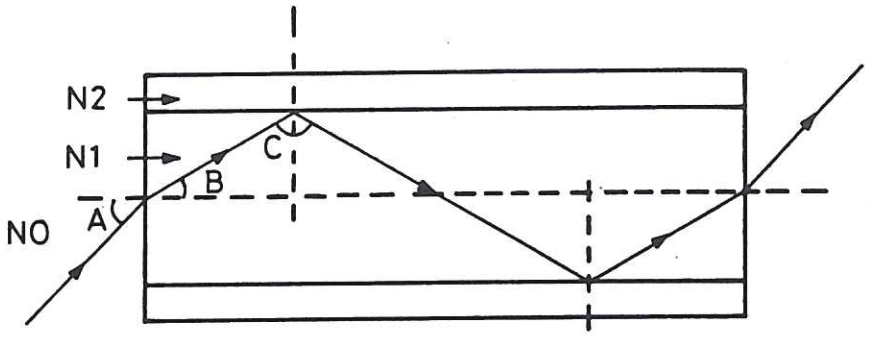

Fig.2. The optical path through the fibre.

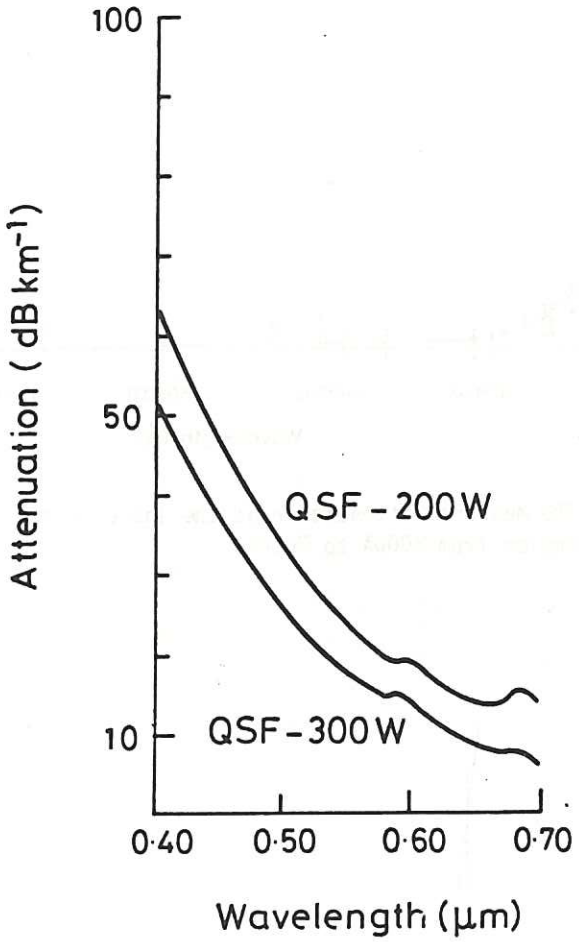

Fig.3. The attenuation of the fibre in the wavelength region from 4000Å to 7000Å.

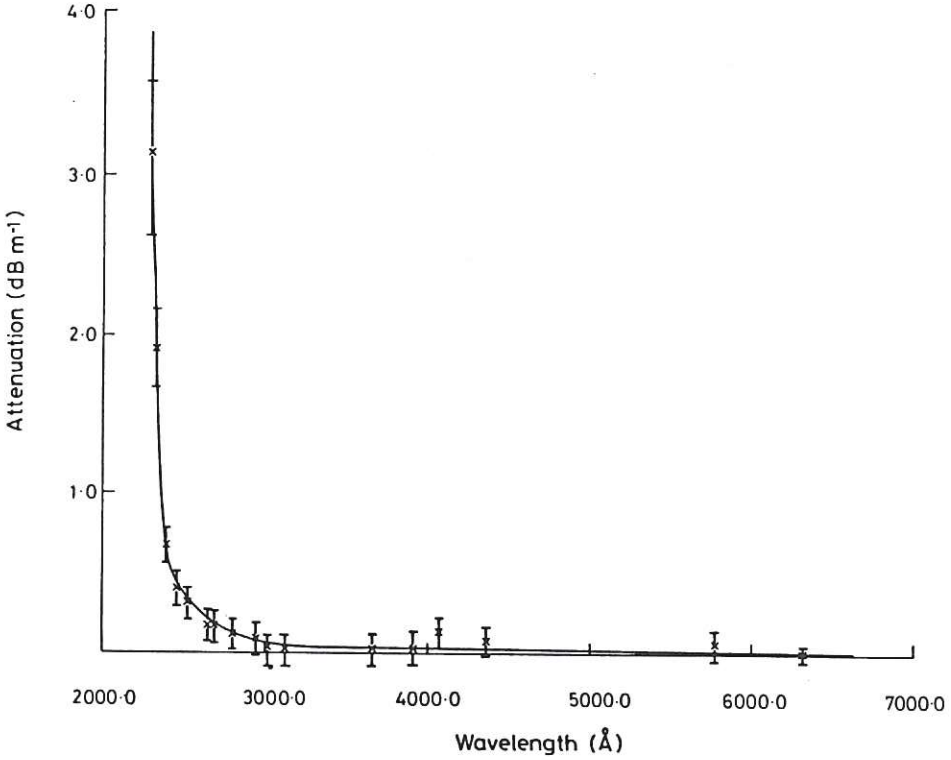

Fig.4. The measured attenuation of the fibre in the wavelength region from 2000Å to 7000Å.

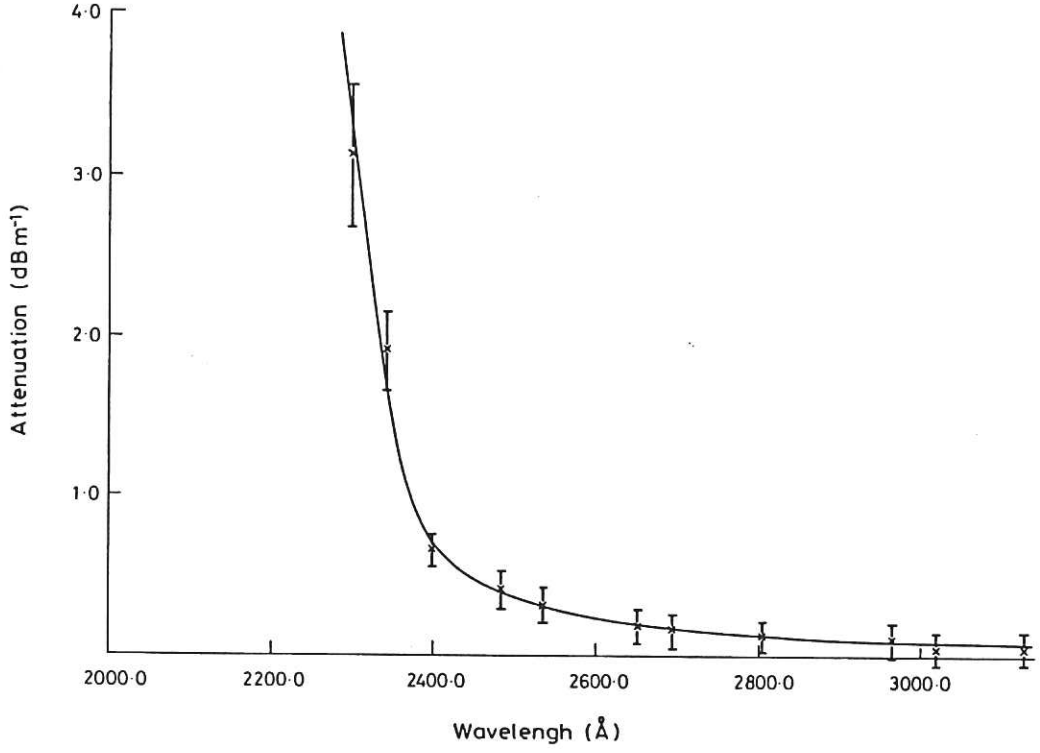

Fig.5. The measured attenuation of the fibre in the wavelength region from 2000Å to 4000Å.

Available from
HER MAJESTY'S STATIONERY OFFICE
49 High Holborn, London, WC1V 6HB
(Personal callers only)
P.O. Box 276, London, SE1 9NH
(Trade orders by post)
13a Castle Street, Edinburgh, EH2 3AR
41 The Hayes, Cardiff, CF1 1JW
Princess Street, Manchester, M60 8AS
Southey House, Wine Street, Bristol, BS1 2BQ
258 Broad Street, Birmingham, B1 2HE
80 Chichester Street, Belfast, BT1 4JY

PRINTED IN ENGLAND